

PROPAGATION PATH PROPERTIES IN ITERATIVE LONGEST-EDGE REFINEMENT

J.P. Suárez¹

A. Plaza¹

G.F. Carey²

¹*University of Las Palmas de Gran Canaria, Canary Islands, Spain,
jsuarez@dcegi.ulpgc.es, aplaza@dma.ulpgc.es*

²*University of Texas at Austin, Austin, Texas, U.S.A. carey@cdfdlab.ae.utexas.edu*

ABSTRACT

In this work we investigate the refinement propagation process in longest-edge based local refinement algorithms for unstructured meshes of triangles. The conformity neighborhood of a triangle, the set of additional triangles that is needed to be refined to ensure mesh conformity is introduced to define the propagation path. We prove that asymptotically the propagation path extends on average to a few neighbor adjacent triangles. We also include numerical evidence which is in complete agreement with the theoretical study reported.

Keywords: mesh refinement, longest edge bisection, propagation path

1. INTRODUCTION

Mesh Generation plays a central role in the Finite Element Method [1, 2, 3], and is a basic tool in many other fields such as Computational Geometry and Computer Graphics. A related problem that is also of considerable interest is refinement of a mesh. The refinement problem can be described as any technique involving the insertion of additional vertices in order to produce meshes with desired features: *well shaped* triangles, *mesh conformity* and *smoothness*. The presence of thin triangles can lead to undesirable behavior affecting numerical stability and accuracy. Mesh conformity refers to the requirement that the intersection of adjacent triangles is either a common vertex or an entire side. Mesh smoothness implies that the transition between small and large elements should be gradual.

Certain longest-edge refinement algorithms [4, 5, 6] guarantee the construction of non-degenerate and smooth unstructured triangulations. In these schemes the longest edges are progressively bisected and hence all angles in subsequent refined triangulations are

greater than or equal to half the smallest angle in the initial triangulation [7]. However, the extent of secondary refinements induced in neighboring¹ elements by the initiating element edge bisection is not known [6, 8]. One can construct pathological cases where refinement of a single element propagates through the entire mesh (Figure 1). However experience indicates that this is an exception and that in practice the refinement propagates through only a few neighbors on average. Our goal here is to address this question. We provide both theoretical results and empirical evidence showing that successive application of refinement to an arbitrary unstructured triangular mesh produces meshes in which the average propagation path is reduced in each refinement stage, and asymptotically approaches the constant 5.

2. PRELIMINARIES. THE REFINEMENT AND THE PROPAGATION PROBLEM

The refinement of triangular meshes involves two main tasks. The first is the partition of the target

¹Throughout this work, neighbor triangles are triangles sharing an edge

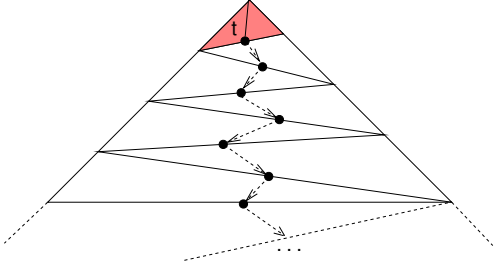


Figure 1: Longest edge refinement propagation. The dependencies in the propagation when refining t are indicated by arrows.

triangles and the second is the propagation to successive neighbor triangles to preserve conformity. Several approaches for partitioning triangles have been studied. The simplest is *Bisection* into two subtriangles by connecting the midpoint of one of the edges to the opposite vertex. If the Longest Edge (LE) is chosen for the bisection, then this is called *Longest Edge Bisection*, see Figure 2 (a). The *Four Triangles Longest Edge Partition*, (*4T-LE*) bisects a triangle into four subtriangles where the original triangle is first subdivided by its longest edge as before and then the two resulting triangles are bisected by joining the new midpoint of the longest edge to the midpoints of the remaining two edges of the original triangle, as in Figure 2 (d), [5].

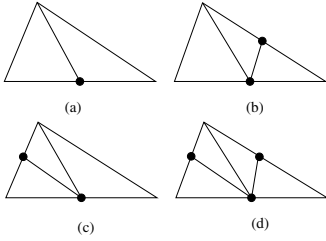


Figure 2: The four possible patterns in the 4T-LE refinement: (a) Bisection in two triangles, (b)-(c) Division in three triangles and (d) Division in four triangles.

In order to ensure the conformity of the arising mesh, the refinement must be extended to additional triangles. This is made for the 4T-LE partition by the use of partial division patterns given in Figure 2 (a)-(c).

Definition 1 (Longest Edge Neighbor triangle) *The longest edge neighbor of a triangle t is the neighbor triangle t^* which shares with t the longest edge of t .*

In the case of an isosceles or equilateral triangle, we may assume a ‘roundoff level’ perturbation to yield a single longest edge. This can be random and hence uniqueness is not implied. However, in the cases in which one of the longest edges has been already identified for bisection in a neighbor triangle, this edge is chosen as the longest edge to get the refinement as local as possible.

Definition 2 (LE Propagation Path [5, 9]) *The Longest Edge Propagation Path (LEPP) of a triangle t_0 is the ordered finite list of all adjacent triangles $LEPP(t_0) = \{t_0, t_1, \dots, t_n\}$ such that t_i is the longest edge neighbor triangle of t_{i-1} .*

Throughout this work τ denotes a 2D conforming triangulation. If longest edge bisection is used to refine a given triangle $t \in \tau$, then the *LEPP*(t) provides the list of triangles to be refined, (see Figure 3). Note that if the 4T-LE partition is used to refine a given triangle t , then the *LEPP*’s of the neighbor triangles of t in the mesh $\tau^* = \tau - t$ provide the lists of triangles to be refined (see Figure 4 and Table 1). As a consequence, the *LEPP*’s provide the main adjacency lists used by the algorithms.

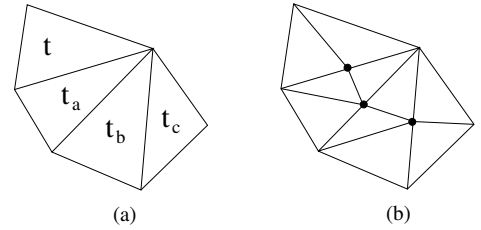


Figure 3: (a) $LEPP(t) = \{t, t_a, t_b, t_c\}$ (b) LE bisection of t and refinement propagation.

Table 1: Triangles and associated LEPP’s of mesh in Figure 4 (a).

Triangle	LEPP	LEPP on $\tau^* = \tau - t$
t	$\{t, t_c, t_d\}$	-
t_a	$\{t_a, t, t_c, t_d\}$	$\{t_a\}$
t_b	$\{t_b, t_e\}$	$\{t_b, t_e\}$
t_c	$\{t_c, t_d\}$	$\{t_c, t_d\}$

Definition 3 (Boundary and Interior triangle) *Let τ be a two dimensional triangulation for a bounded domain Ω . A triangle $t \in \tau$ is said to be a boundary triangle if t has an edge coincident with the boundary $\partial\Omega$ of Ω . Otherwise, t is an interior triangle of τ .*

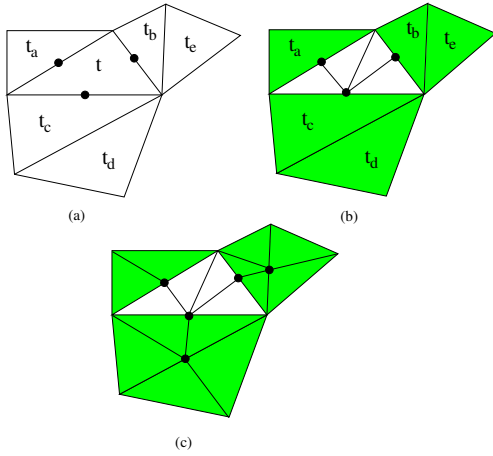


Figure 4: (a) Edge bisection for refining triangle t (b) 4T-LE refinement of t , (c) refinement of triangles.

Definition 4 (Pair of Terminal triangles) *Two neighbor triangles (t, t^*) will be called a ‘pair’ of terminal triangles if they share a common longest edge. If a triangle t does not belong to a pair of terminal triangles, t is said to be a ‘single’ triangle.*

For any triangle t_0 , if $LEPP(t_0) = \{t_0, \dots, t_{n-1}, t_n\}$ then for triangle t_n either: (i) t_n has its longest edge coincident with the boundary or (ii) t_{n-1} and t_n are a pair of terminal triangles that share a common longest edge, [9].

If all the triangles in a mesh are pairs of terminal triangles, then all the $LEPP$ lists are comprised only of two triangles.

Definition 5 (LEPP-balanced mesh) *Triangulation τ is said to be LEPP-balanced if it is comprised of pairs of terminal triangles. Otherwise, it is said to be a non LEPP-balanced mesh.*

Remark: In [10] the terminology ‘balanced’ is applied to angles and areas. This is relevant to triangle shape but not directly related to our $LEPP$ study here.

Definition 6 (LEPP-balancing degree) *Let τ contain N triangles of which T triangles are in pairs of terminal triangles. Then, the LEPP-balancing degree of τ , noted as $B(\tau)$, is defined as follows:*

$$B(\tau) = \frac{T}{N} \quad (1)$$

Note that $0 \leq B(\tau) \leq 1$ and in the case $B(\tau) = 1$, the mesh is LEPP-balanced.

Remark: If τ is such that the LEPP-balancing degree is 0, then the conformity process when refining any triangle $t_0 \in \tau$ extends to the boundary of τ .

Figure 5 shows a LEPP-balanced mesh in (a) and a non balanced mesh in (b). Here and in subsequent figures we represent the longest-edges with a dashed line.

A simple example of a LEPP-balanced mesh is any mesh comprised entirely of pairs of right triangles sharing the longest-edges. In such a mesh, if one applies uniform 4T-LE refinement, then all triangles are pairs of terminal triangles and they are similar to the original right triangles.

3. PROPAGATION PROPERTIES OF RECURSIVE 4T-LE REFINEMENT

We are particularly interested in the average and maximum lengths of the propagation paths generated by longest-edge refinement since they are important in assessing algorithm efficiency.

First we introduce the *Conformity Neighborhood* associated with the application of 4T-LE local refinement. This concept will be useful in the study of the propagation properties.

Definition 7 (Conformity Neighborhood V_c) *When refining a triangle $t \in \tau$, the Conformity Neighborhood $V_c(t)$ of t , is the set of triangles in $\tau^* = \tau - t$ that need to be refined due to the conformity process for t .*

Definition 8 (M1) *When refining a triangle $t \in \tau$, $M1(t)$ is said to be the size of $V_c(t)$: $M1(t) = |V_c(t)|$.*

Note that $M1(t)$ measures the extent of the propagation refinement zone for triangle t , in number of triangles.

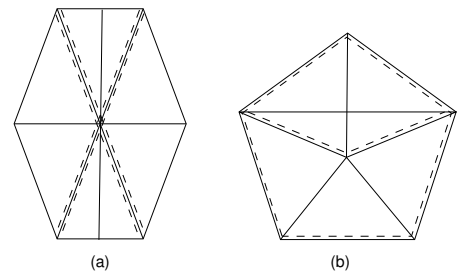


Figure 5: (a) LEPP-Balanced mesh, (b) Non balanced LEPP mesh.

Proposition 1 For each $t \in \tau$, $M1(t)$ is the sum of the lengths of the LEPP's of the neighbors of t in the mesh $\tau^* = \tau - t$. \square

Figure 1 shows that it always is possible to construct meshes in which $M1(t)$ is $\mathcal{O}(N)$, where N is the number of elements. Here, the average of $M1$ is $\mu(M1) = \frac{\sum_t M1(t)}{N} = \frac{\sum_{k=0}^{N-1} k}{N} = \frac{\frac{N-1}{2} \cdot N}{N} = \frac{N-1}{2}$. On the other hand, if $B(\tau) = 1$ as in Figure 5 (a), then $M1(t) \leq 5 \forall t \in \tau$.

Definition 9 (M2) For each $t \in \tau$, $M2(t)$ is the maximum length of the LEPP's of the neighbor triangles of t in the mesh $\tau^* = \tau - t$: $M2 = \max\{|V_c(t) \cap LEPP(t_a)|, t_a \text{ neighbor to } t\}$.

Since the conformity process extends at most by the three edges of t the propagation defines at most three lists of ordered triangles. $M2(t)$ is the maximum number of triangles of the three resulting lists. For example, in Figure 4, $M2(t) = 2$ because the maximum number of triangles among $\{t_b, t_e\}$, $\{t_c, t_d\}$, $\{t_a\}$ is 2, see Table 1.

Proposition 2 Let τ be LEPP-balanced. Then, for each interior triangle $t \in \tau$, $M1(t) = 5$ and $M2(t) = 2$.

Proof:

Let t be an interior triangle of τ . Since τ is a LEPP-balanced mesh, t is adjacent to another triangle t_1 by their common longest edge. Let t_2 and t_3 be the two other adjacent triangles to t . Again, since τ is a LEPP-balanced mesh, t_2 and t_3 are adjacent to other triangles t'_2 and t'_3 by their respective common longest edges, and $t'_2 \neq t \neq t'_3$. Considering the mesh $\tau^* = \tau - t$ we have that $LEPP(t_1) = \{t_1\}$, $LEPP(t_2) = \{t_2, t'_2\}$ and $LEPP(t_3) = \{t_3, t'_3\}$. Hence $V_c(t) = \{t_1, t_2, t_3, t'_2, t'_3\}$ so $M1(t) = 5$ and $M2(t) = 2$. \square

Our next goal is to prove that the uniform application of the 4T-LE partition will produce a sequence of meshes with increasing LEPP-balancing degree approaching 1. We shall also prove that the mean of $M1$ and the mean of $M2$ tend to 5 and 2 respectively, when the number of refinements applied tends to infinity.

Proposition 3 [4] (a) The first application of the 4T-LE partition to a given triangle t_0 introduces two new triangles that are similar to the original triangle

t_0 . Moreover, these two triangles have their longest edges coincident with the longest edge of the original triangle. The remaining two new triangles t_1 , are similar to each other but not necessarily to the original triangle t_0 . Triangles t_1 may be a terminal pair or not.

(b) The iterative application of the 4T-LE partition to a given triangle t_0 introduces at most one new distinct (up to similarity) triangle in each iteration.

Proof:

The proof follows from the angle properties of similar subtriangles obtained by 4T-LE quadrisection as seen in Figures 6 and 7 for the acute and obtuse triangles respectively. \square

Proposition 4 If the 4T-LE partition to an initial triangle t_0 introduces a pair of terminal triangles t_1 , then the iterative application of the 4T-LE partition introduces pairs of terminal triangles excepting the triangles located at the longest edge of t_0 . Moreover, in this case only two classes of similar triangles are generated, corresponding to t_0 and t_1 respectively (see Figure 6).

Proof:

The hypothesis of Proposition 4 is depicted in Figure 6 (b). The proof follows trivially from the angle properties of parallel lines in the nested triangles. \square

To demonstrate that recursive uniform 4T-LE refinement introduces meshes with relatively more pairs of terminal triangles for any arbitrary triangular mesh we consider right, acute and obtuse triangles respectively. We begin in the next Proposition with the right and acute triangle cases:

Proposition 5 (Right and acute triangle cases) The application of the 4T-LE partition to an initial right or acute triangle t_0 produces two new single triangles similar to the original one (located at the longest edge of t_0) and a pair of terminal triangles t_1 . These triangles t_1 are also similar to the original one t_0 in the case of right triangle t_0 , and they are similar to each other but non-similar to the initial one in the case of acute triangle t_0 . (See Figure 6). \square

The obtuse triangle case offers a different situation:

Proposition 6 (Obtuse triangle case) The application of the 4T-LE partition to an initial obtuse triangle t_0 , produces two new single subtriangles similar to the original one (located at the longest edge of t_0) and a pair of subtriangles t_1 . These subtriangles t_1 either

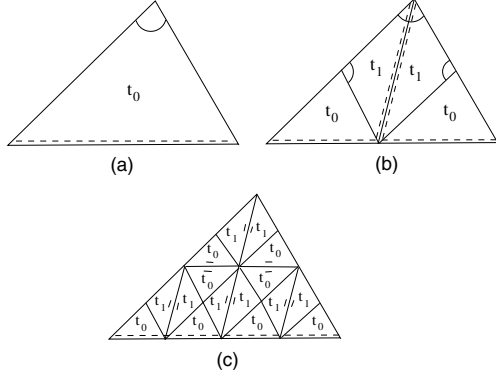


Figure 6: 4T-LE partition. Acute triangle.

1. are a pair of similar terminal triangles, as in Figure 6 (b) (t_0 is said to be a Type 1 obtuse triangle), or
2. a pair of similar single triangles, as in Figure 7 (b) (t_0 is said to be a Type 2 obtuse triangle).

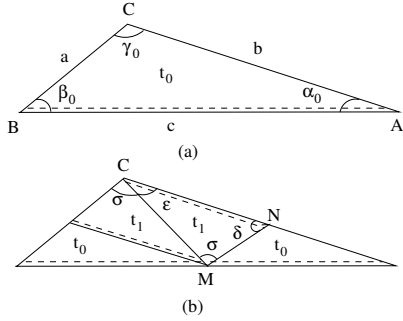


Figure 7: (a) Type 2 obtuse triangle t_0 (b) 4T-LE partition of t_0 .

Proof:

Let $\alpha_0 \leq \beta_0 \leq \gamma_0$ be the angles of the initial obtuse triangle t_0 and let a, b, c be the sides of t_0 respectively opposite to α_0, β_0 and γ_0 . For the new non-similar subtriangles generated, we denote by ϵ the opposite angle to MN and σ the opposite angle to CN . Since $MN \leq CN$ and $\epsilon \leq \sigma$ the longest edge of t_1 is either the new edge CM or CN . In the first situation (point 1 of the Proposition), triangles t_1 are a pair of terminal triangles sharing edge CM as the longest edge.

In the second case, the largest angle of t_1 is σ (see triangles t_1 in Figure 7). The new triangles t_1 are not a pair of terminal triangles (point 2 of the Proposition). \square

It should be noted that the 4T-LE partition always produces two new single triangles similar to the original one (located at the longest edge of t_0) and excepting for Type 2 obtuse triangles, a pair of terminal triangles (similar or non similar to the original one). Moreover, in this scenario, the single triangles generated by the iterative 4T-LE partition are those located at the longest edge of the initial triangle, Proposition 4 (see Figure 6).

The following Proposition states the recursive improvement property of the 4T-LE partition for obtuse triangles [4]:

Proposition 7 *If the 4T-LE partition of an obtuse triangle t_0 introduces a pair of similar single triangles t_1 of largest angle γ_1 , then*

1. $\gamma_1 = \sigma$
2. $\gamma_1 = \gamma_0 - \epsilon \leq \gamma_0 - \alpha_0$

hold for the new angles of the new triangle t_1 , see Figure 7. \square

It is worth noting, in relation to Proposition 7 above, that after a finite number of applications of the 4T-LE partition to triangle t_0 and its successors a non-obtuse triangle is obtained. This is a straightforward consequence of statement 2 in Proposition 7. Furthermore, after a first non-obtuse triangle is obtained then the successive application of the 4T-LE partition does not generate new non-similar triangles.

In view of the previous properties, we have:

Proposition 8 *Let $\Gamma = \{\tau_0, \tau_1, \dots, \tau_n\}$ be a sequence of nested meshes obtained by repeated application of 4T-LE partition to the previous mesh. Then, the LEPP-balancing degree of the meshes tends to 1 as $n \rightarrow \infty$.*

Proof:

It suffices to prove the result for the case in which the initial mesh τ_0 only contains a single triangle t_0 . Then, the number of generated triangles associated with the 4T-LE partition at stage n of refinement is:

$$N_n = 4^n \quad (2)$$

First, we prove the proposition for initial right, acute, and the Type 1 obtuse triangles. In this situation, the number of triangles in pairs of terminal triangles

T_n generated at stage n of uniform $4T$ -LE partition satisfies (see Proposition 4 and Figure 6):

$$T_n = 4T_{n-1} + 2(N_{n-1} - T_{n-1}) = 2(T_{n-1} + N_{n-1}) \quad (3)$$

with $N_0 = 1$ and $T_0 = 0$.

Solving the recurrence relations 2, 3 we get:

$$T_n = 4^n - 2^n \quad (4)$$

Therefore,

$$\lim_{n \rightarrow \infty} B(\tau_n) = \lim_{n \rightarrow \infty} \frac{T_n}{N_n} = 1$$

To complete the proof, we now consider the case of an initial Type 2 obtuse triangle t_0 . Table 2 presents the number of distinct types of triangles generated by the $4T$ -LE iterative refinement of t_0 . We denote by t_j^n the number of triangles of similarity class t_j , $j = 0, 1, 2, \dots, k$ at stage n of refinement. For example, after the second refinement 4 triangles are similar to t_0 , 8 triangles similar to t_1 and 4 new triangles similar to t_2 .

From Proposition 6 (2) and Figure 7 we derive Table 2, in which the following relation holds:

$$t_j^n = 2(t_j^{n-1} + t_{j-1}^{n-1}), \quad j = 1, 2, 3, \dots, k \quad (5)$$

The solution to Equation (5) with initial condition $t_0^0 = 1$ can be easily expressed in terms of binomial coefficients as follows:

$$t_j^n = 2^n \binom{n}{j} \quad (6)$$

On the other hand, from Proposition 7, the iterative $4T$ -LE partition of any obtuse triangle t_0 produces a finite number of distinct (up to similarity) triangles, t_j^i , $0 < j \leq k$. After k refinement stages there will no longer be distinct new generated triangles different from those already generated, (see proof of Proposition 6). Therefore, the number of triangles in pairs of terminal triangles T_n after the k refinement stage with $n > k$ satisfy:

$$T_n \geq 2^n \sum_{m=k}^n \binom{n}{m}$$

It follows that:

$$1 \geq B(\tau_n) \geq \frac{2^n \sum_{m=k}^n \binom{n}{m}}{2^n \sum_{m=0}^n \binom{n}{m}} = \frac{\sum_{m=k}^n \binom{n}{m}}{2^n}$$

Table 2: Triangle evolution in the $4T$ -LE partition.

Ref.	0	1	2	3	4	...	k	...	n
t_0	1	2	4	8	16	...	t_0^k	...	t_0^n
t_1		2	8	24	64	...	t_1^k	...	t_1^n
t_2			4	24	96	...	t_2^k	...	t_2^n
t_3				8	64	...	t_3^k	...	t_3^n
t_4					16	...	t_4^k	...	t_4^n
...					
t_k						...	t_k^k	...	t_k^n

Taking limits:

$$1 \geq \lim_{n \rightarrow \infty} B(\tau_n) \geq \lim_{n \rightarrow \infty} \frac{2^n \sum_{m=k}^n \binom{n}{m}}{2^n \sum_{m=0}^n \binom{n}{m}}$$

Since

$$\sum_{m=k}^n \binom{n}{m} = 2^n - \sum_{m=0}^{k-1} \binom{n}{m} \geq 2^n - \binom{n}{k-1} k$$

we have

$$1 \geq \lim_{n \rightarrow \infty} B(\tau_n) \geq \lim_{n \rightarrow \infty} \frac{2^n - \binom{n}{k-1} k}{2^n} = 1$$

So, $\lim_{n \rightarrow \infty} B(\tau_n) = 1$. □

Proposition 9 For iterative application of $4T$ -LE uniform refinement to an initial triangular mesh τ_0 , the means of M1 and of M2 tend to 5 and 2 respectively, as the number of refinements tend to infinity.

Proof:

If the initial mesh is LEPP-balanced the result is trivial. Let us suppose that the initial mesh contains non-terminal triangle.

In any subsequent mesh we have pairs of terminal triangles and non terminal triangles. First, we prove the proposition for any right, acute, or Type 1 obtuse non terminal triangles arranged in such a way that M1 and M2 are the largest. That is, all the non-terminal triangles constitute a unique LEPP. Figure 8 (a) reproduces a possible situation within a mesh. After a few refinement steps it is observed that new non terminal triangles are located at the longest edges of the initial triangles. We represent in bold the longest edges of non terminal triangles as shown in Figure 8 (d) and call here *polyline*.

Non terminal triangles have their longest edges on the polyline, see Figure 8 (d). Among them, those having

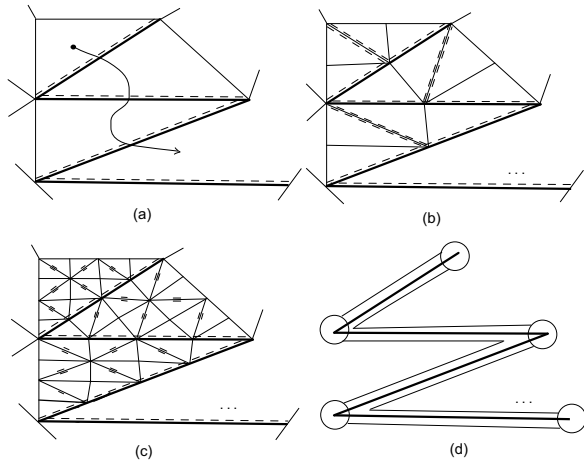


Figure 8: (a) Non terminal triangles forming a LEPP. (b)-(c) 4T-LE refinement of triangulation in (a). (d) longest edges of triangles in (a).

a vertex at the polyline show $M1 = 7$ and $M2 = 3$. For a terminal triangle we get either $5 \leq M1 \leq 6$ or $2 \leq M2 \leq 3$ if it has a vertex on the polyline, or $M1=5$ and $M2=2$ otherwise. After n refinement steps, the number of non terminal triangles is $X_n = 2^n X_0$ and the number of total triangles is $N_n = 4^n N_0$. Hence, upper and lower bounds for the average of $M1$ are as follows:

$$\frac{6X_n + 5(N_n - X_n)}{N_n} \leq M1 \leq \frac{7 \cdot 2X_n + 5(N_n - 2X_n)}{N_n}$$

Similarly for $M2$:

$$\frac{2X_n + 2(N_n - X_n)}{N_n} \leq M2 \leq \frac{3 \cdot 2X_n + 2(N_n - 2X_n)}{N_n}$$

Taking limits we find that the means of $M1$ and of $M2$ tend to 5 and 2 respectively, as the number of refinements n tends to infinity.

To complete the proof, we should also consider the case of Type 2 obtuse triangles. As pointed out after Proposition 7, in repeated 4T-LE refinement, largest angles of Type 2 obtuse triangles clearly decrease, and after a finite number k of 4T-LE partitions the new generated triangles will be no longer obtuse. Hence, the first part of the proof for right or acute triangle cases then applies. \square

4. NUMERICAL EXPERIMENTS

In this section we present numerical results showing that the practical behavior of the 4T-LE partition is in concordance with the reported theory in this work,

mainly Propositions 8 and 9.

We next consider a Delaunay mesh in a rectangle (Figure 9 (a)) and an irregular mesh in a pentagon (Figure 12 (a)) with five stages of uniform refinement. It should be noted that the triangles in the Delaunay mesh are almost regular in terms of the angles moreover, the mean of the minimum angles and of the maximum angles are 48.91 and 72.91 degrees respectively. The initial value of $B(\tau_0)$ is 0.4833. On the other hand, for the irregular mesh in the pentagon the mean of the minimum angles and of the maximum angles are 9.18 and 120.41 degrees respectively, and $B(\tau_0) = 0$.

The refined meshes for the initial Delaunay mesh are presented in Figures 9 (b)-(d). The light shading in Figures 9 and 12 illustrate the triangles in terminal pairs. In Table 3 it can be noted that the number of triangles in terminal pairs increase as the refinement stage grows, and as result, so does the LEPP-balancing degree. Table 4 reports the means and standard deviations of $M1$ and $M2$ and respective histograms are graphed in Figure 11. It is observed that both means tend to 5 and 2 respectively, as the refinement continues. The asymptotic behavior is graphed in Figure 10.

Similarly, the refined meshes for the ‘pentagonal’ domain are shown in Figure 12 and the asymptotic behavior for the means $\mu(M1)$, $\mu(M2)$ graphed in Figure 13. The evolution of the LEPP-balancing degree is summarized in Table 5 and a comparison graphed in Figure 15. Note that in both meshes the LEPP-balancing degree tends to 1 when the number of refinements increases, even in the Pentagonal mesh, which exhibits an initial LEPP-balancing degree $B(\tau_0) = 0$ (see Figure 15). Table 6 reports the means and standard deviations of $M1$ and $M2$ and respective histograms are graphed in Figure 14.

These results are also applicable to local refinement. In order to empirically demonstrate this we consider application of 4T-LE local refinement on a domain corresponding to the Gran Canaria Island (Figure 16). The initial mesh is a Delaunay mesh and one refinement step is applied on respective disjoint subregions S_1 , S_2 and S_3 with $S = S_1 \cup S_2 \cup S_3$, for innermost region S_3 , intermediate region S_2 and outermost region S_1 . Table 7 and Figure 17 confirm similar behavior to that observed for uniform refinement with $\mu(M1)$ and $\mu(M2)$ approaching 5 and 2 respectively and the LEPP-balancing degree approaching 1. Figure 18 graphs $M1$ and $M2$ histograms for the initial mesh and refinement steps 3 and 6.

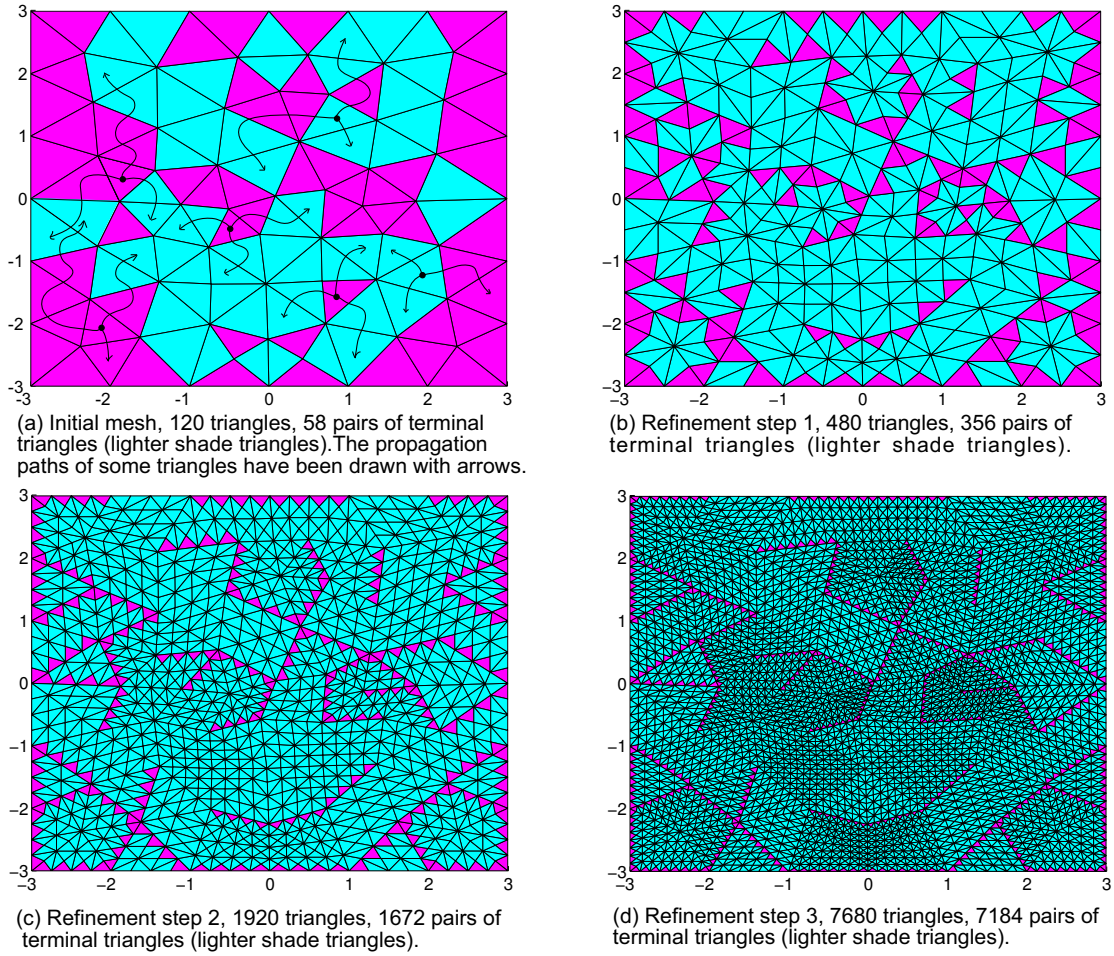


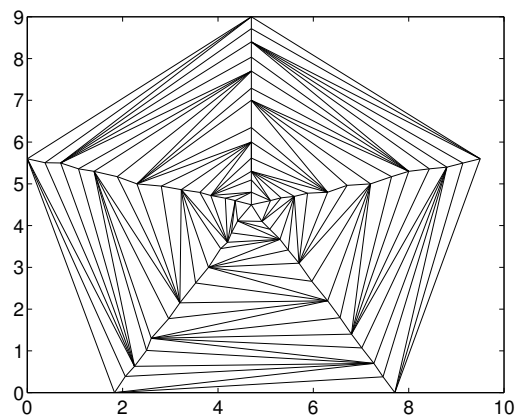
Figure 9: Delaunay mesh. Uniform 4T-LE refinement.

Table 3: Statistics for the refinement of the Delaunay mesh (Figure 9). R=Refinement step, T=Triangles in Terminal Pairs, N=Triangles, B=LEPP-Balancing Degree.

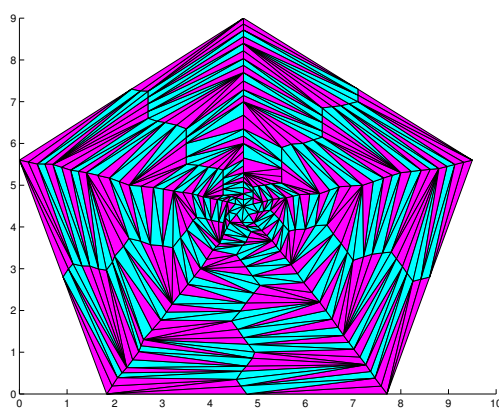
R	T	N	B
0	58	120	0.48333
1	356	480	0.74166
2	1672	1920	0.87083
3	7184	7680	0.93541
4	29728	30720	0.96770
5	121447	122880	0.98821

Table 4: M1 and M2 statistics for the refinement of the Delaunay mesh (Figure 9). Average (μ) and Standard Deviation (σ).

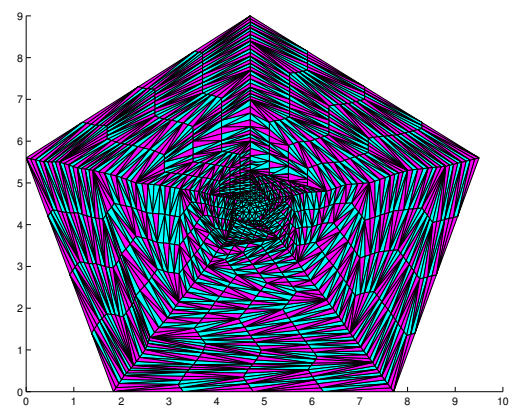
R	N	$\mu(M1)$	$\mu(M2)$	$\sigma(M1)$	$\sigma(M2)$
0	120	5.233	2.625	1.873	0.888
1	480	5.112	2.381	1.135	0.582
2	1920	5.057	2.195	0.772	0.421
3	7680	5.028	2.096	0.535	0.303
4	30720	5.014	2.048	0.374	0.216
5	122880	5.007	2.028	0.275	0.040



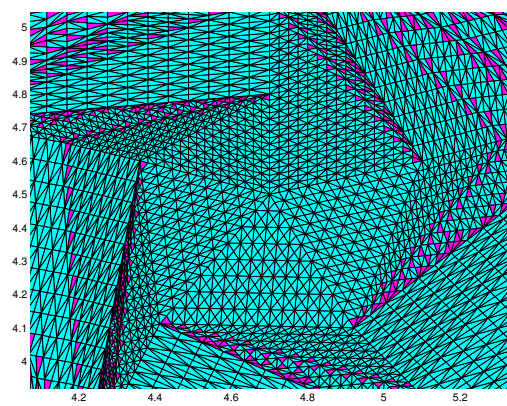
(a) Initial mesh, 0 terminal triangles, 125 triangles.



(b) Refinement step 1, 246 terminal triangles (lighter shade triangles), 500 triangles.



(c) Refinement step 2, 1088 terminal triangles (lighter shade triangles), 2000 total triangles.



(d) Refinement step 3, 4778 terminal triangles (lighter shade triangles), 8000 triangles (interior zoom).

Figure 12: Pentagonal mesh. Uniform 4T-LE refinement.

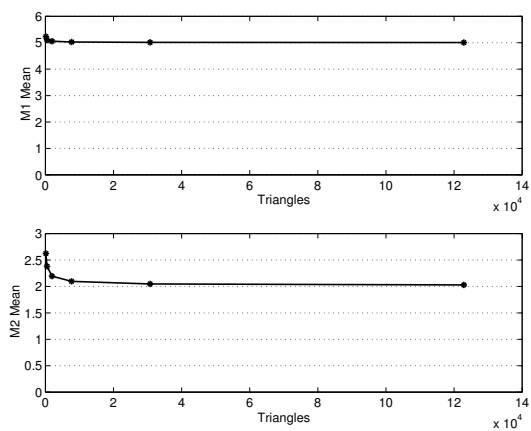


Figure 10: Evolution of $\mu(M1)$ and $\mu(M2)$ for the refinement of the Delaunay mesh (Figure 9).

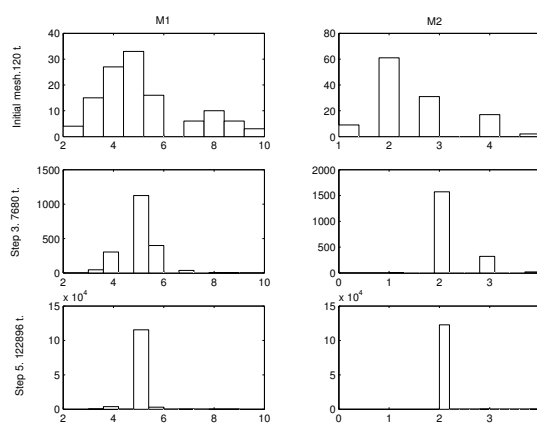


Figure 11: M1 and M2 histograms for the refinement of the Delaunay mesh (Figure 9).

Table 5: Statistics for the refinement of the Pentagonal mesh (Figure 12). R=Refinement step, T=Triangles in Terminal Pairs, N=Triangles, B=LEPP-Balancing Degree.

R	T	N	B
0	0	125	0
1	246	500	0.49200
2	1088	2000	0.54400
3	4778	8000	0.59725
4	21240	32000	0.66375
5	103970	128000	0.81230

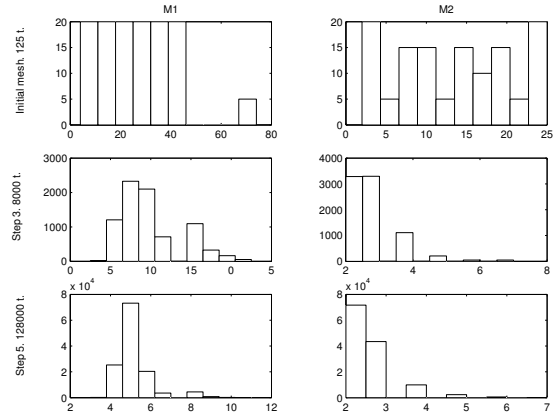


Figure 14: M1 and M2 histograms for the refinement of the Pentagonal mesh (Figure 12).

Table 6: M1 and M2 statistics for the refinement of the Pentagonal mesh (Figure 12). Average (μ) and Standard Deviation (σ).

R	N	$\mu(M1)$	$\mu(M2)$	$\sigma(M1)$	$\sigma(M2)$
0	125	26.544	14.392	16.569	7.156
1	500	6.910	3.800	2.204	1.668
2	2000	6.200	3.048	1.699	1.103
3	8000	5.997	2.831	1.553	0.883
4	32000	5.482	2.412	1.122	0.800
5	128000	5.370	2.204	0.947	0.757

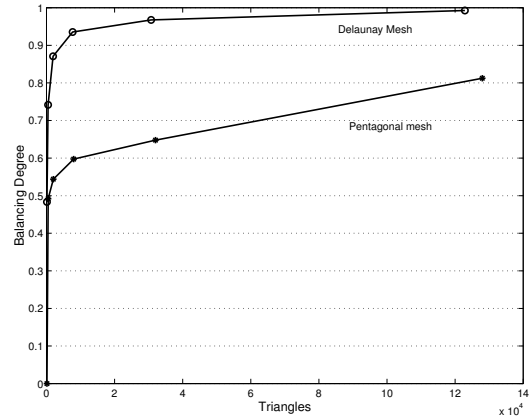


Figure 15: LEPP-balancing degree evolution for the refinement of Delaunay and Pentagonal meshes.

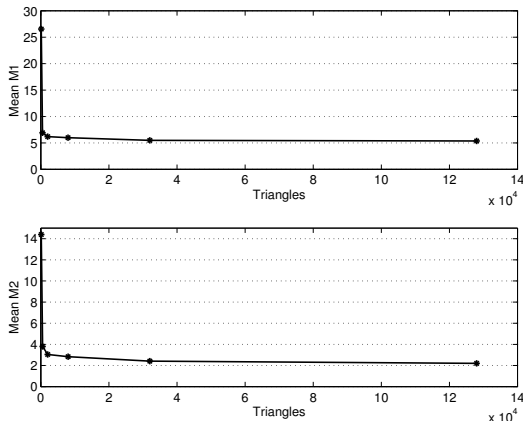
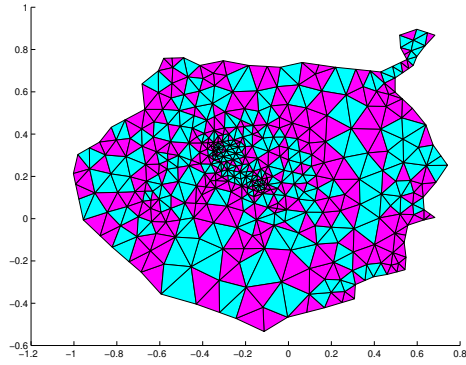


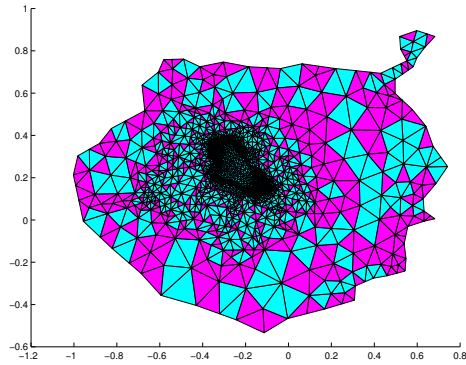
Figure 13: Evolution of $\mu(M1)$ and $\mu(M2)$ for the refinement of the Pentagonal mesh (Figure 12).

Table 7: M1 and M2 statistics for the refinement of the Gran Canaria mesh (Figure 16). Average (μ) and Standard Deviation (σ).

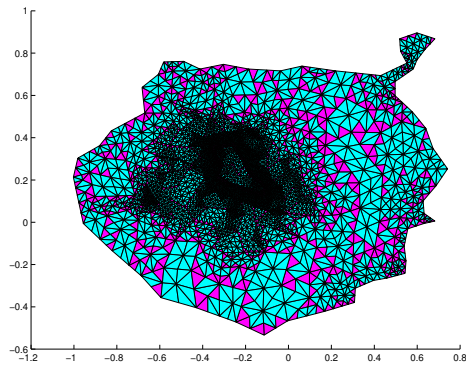
R	N	$\mu(M1)$	$\mu(M2)$	$\sigma(M1)$	$\sigma(M2)$
0	592	6.619	3.451	2.764	1.660
1	736	6.690	3.539	2.577	1.663
2	1230	6.505	3.383	2.265	1.601
3	2624	6.019	2.918	1.679	1.051
4	9258	5.513	2.426	1.162	0.601
5	30730	5.247	2.367	0.681	0.509
6	41448	5.212	2.189	0.564	0.328



(a) Refinement step 1, 326 terminal triangles (lighter shade triangles), 736 total triangles.



(b) Refinement step 3, 1588 terminal triangles (lighter shade triangles), 2624 total triangles.



(c) Refinement step 4, 7020 terminal triangles (lighter shade triangles), 9258 total triangles.

Figure 16: Gran Canaria mesh. Local 4T-LE refinement.

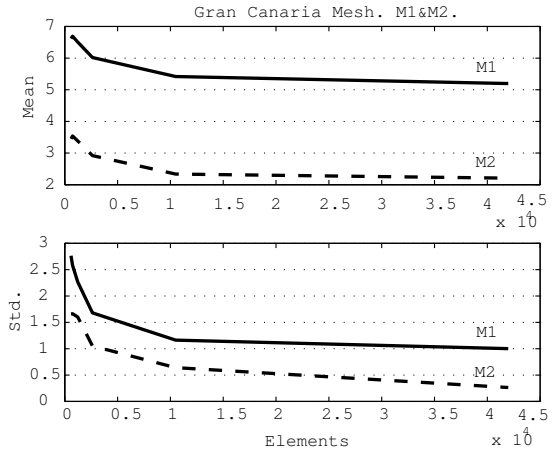


Figure 17: M1 and M2 evolution for the refinement of the Gran Canaria mesh (Figure 16).

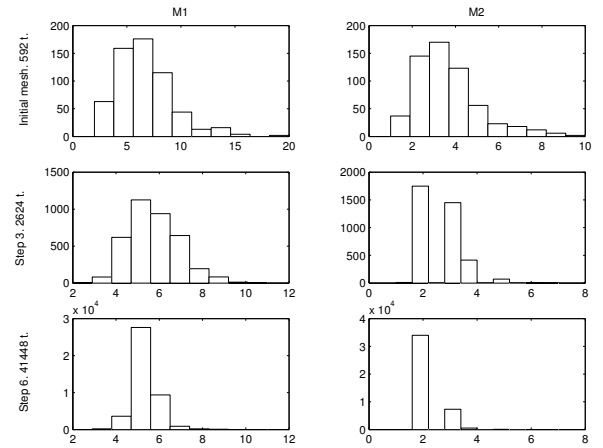


Figure 18: M1 and M2 histograms for the refinement of the Gran Canaria mesh (Figure 16).

Table 8: Statistics for the refinement of the Gran Canaria mesh (Figure 16). R=Refinement step, T=Triangles in Terminal Pairs, N=Triangles, B=LEPP-Balancing Degree.

R	T	N	B
0	248	592	0.41891
1	326	736	0.44293
2	672	1230	0.54634
3	1588	2624	0.60518
4	7020	9258	0.75826
5	26282	30730	0.85525
6	35746	41448	0.86243

5. CONCLUSIONS

In this work we have studied the propagation problem associated with longest edge based refinement algorithms in 2D. We have theoretically proved in the paper that the propagation path asymptotically extends on average to a few neighbor adjacent triangles. This result has also been numerically demonstrated for repeated local refinement. The extent of refinement for triangle t defines a Conformity Neighborhood characterized by two parameters ($M1(t)$ and $M2(t)$).

When repeated uniform refinement is applied to an initial arbitrary triangular mesh, the average of the parameters $M1(t)$ tends to 5 and the average of $M2(t)$ tends to 2. This implies for local refinement of practical applications that on average the propagation of secondary refinements induced by specified refinements will be limited to a proportionally small number of elements with a confined limit. In view of this, an asymptotic estimate of the cost is easily determined: since the cost of refinement of a single triangle is bounded by a small constant c and the number of triangles in the conformity neighborhood of any such triangle is 5 on average, the asymptotic estimate of the cost to refine a triangle is obviously $6c$.

We also have introduced the concept of LEPP-balancing degree (ratio between triangles in terminal pairs and total triangles in a mesh) for longest edge refinement of meshes and have proved that the LEPP-balancing degree asymptotically tends to 1. These results are also a global measure of the improvement of the generated meshes on the size of the conformity neighborhood.

The counterpart 3D propagation problem needs a more complex study because the number of connectivity patterns are considerably higher than in 2D. It should be noted that the 4T-LE refinement uses three partial division patterns while the extension to three dimensions, the 8T-LE partition may involve more than fifty partial divisions for the sake of conformity [11]. We have made some exploratory numerical studies of LEPP behavior for refinement of tetrahedral meshes and this topic is the subject of our continuing work

Acknowledgements

This research has been partially supported by Sandia grant #56522 and ULPGC grant UNI2002/22.

References

- [1] Bern M., Plassmann P. "Mesh Generation", *Handbook of Computational Geometry*, pp. 291–332, 2000
- [2] Canann S., Saigal S., Owen S., Eds. "Special Edition on Unstructured Mesh Generation." *International Journal for Numerical Methods in Engineering*, vol. 1, no. 49, 2000
- [3] Carey G. *Computational Grids: generation, adaptation and solution strategies*. Taylor & Francis, 1997
- [4] Rivara M., Iribarren G. "The 4-triangles longest-side partition of triangles and linear refinement algorithms." *Mathematics of Computation*, vol. 65, no. 216, 1485–1502, 1997
- [5] Rivara M. "Mesh refinement based on the generalized bisection of simplices." *SIAM Journal of Numerical Analysis*, vol. 2, 604–613, 1984
- [6] Rivara M., Venere M. "Cost analysis of the longest-side (triangle bisection) refinement algorithm for triangulation." *Engineering with Computers*, vol. 12, 224–234, 1996
- [7] Rosenberg I., Stenger F. "A lower bound on the angles of triangles constructed by bisecting the longest side." *Mathematics of Computation*, vol. 29, 390–395, 1975
- [8] Jones M., Plassmann P. "Parallel algorithms for adaptive mesh refinement." *SIAM Journal in Scientific Computing.*, vol. 18, 686–708, 1997
- [9] Rivara M. "New mathematical tools and techniques for the refinement and/or improvement of unstructured triangulations." *Proceeding 5th International Meshing Roundtable'96. SANDIA Report SAND 96-2301*, pp. 77–86. 1984
- [10] Dai Y., Katoh N., Cheng S.W. "LMT-skeleton heuristics for several new classes of optimal triangulations." *Computational Geometry*, vol. 17, 51–68, 2000
- [11] Plaza A., Padrón M., Carey G. "A 3D refinement/derefinement combination to solve evolution problems." *Applied Numerical Mathematics*, vol. 32, no. 4, 285–302, 2000